Flexible optical amplifier for visible light communications based in organic-inorganic hybrids

Ana Bastos[1,2], Barry McKenna[3], Mário Lima[2], Paulo S. André[4], Luís D. Carlos[1], Rachel C. Evans[5] and Rute A. S. Ferreira[1,]*

[1]Department of Physics, CICECO - Aveiro Institute of Materials, University of Aveiro, Campus Universitário de Santiago, 3810-193 Aveiro, Portugal
[2]Department of Electronics, Telecommunications and Informatics, Instituto de Telecomunicações, University of Aveiro, Campus Universitário de Santiago, 3810-193 Aveiro, Portugal
[3]School of Chemistry, Trinity College Dublin, Dublin 2, Ireland
[4]Instituto de Telecomunicações and Department of Electric and Computer Engineering, Instituto Superior Técnico, Universidade de Lisboa, Av. Rovisco Pais, 1049-001 Lisbon, Portugal
[5]Department of Materials Science & Metallurgy, University of Cambridge, 27 Charles Babbage Road, Cambridge CB3 0FS, U.K.

Supporting Information

Table and figure captions

Table S1 Composition, processing method and thickness of PBS-di-ureasils prepared in this study. [PBS-PFP] is the concentration of the stock PBS-PFP solution (in μM repeat units, r.u.), that is added to the d-UPTES. The weight percent (wt%) of polymer incorporated was estimated from [PBS-PFP] and the resultant mass of the dry CPE-di-ureasil.

Figure S1. Ellipsometric parameters I_s (open circles) and I_c (open triangles) measured for (a) dU(600)-M; (b) PBS1-M; (c) PBS2-M; (d) dU(600)-F; (e) PBS3-F; (f) PBS4-F; and (g) PBS5-F. The solid lines represent the data best fit.

Figure S2. Ellipsometric parameters I_s (open circles) and I_c (open triangles) measured in PBS1-M in the regions exposed to UV radiation with energy of (a) 30; (b) 60; (c) 80; (d) 100; (e) 120 μJ·pulse^{-1}. The solid lines represent the data best fit.

Figure S3. Ellipsometric parameters I_s (open circles) and I_c (open triangles) measured in PBS2-M in the regions exposed to UV radiation with energy of (a) 30; (b) 60; (c) 80; (d) 100; (e) 120 μJ·pulse^{-1}. The solid lines represent the data best fit.

Figure S4. Dispersion curves obtained for the channel waveguide regions in PBS1-M.

Figure S5. Emission spectra for different stripe lengths in (a) dU(600), (b) PBS1-M.

Figure S6. Emission spectra for different stripe lengths PBS1-M in the regions exposed to UV radiation with energy of (a) 30; (b) 60; (c) 80; (d) 100; (e) 120 μJ·pulse^{-1}.

Figure S7. Emission spectra for different stripe lengths PBS2-M in the regions exposed to UV radiation with energy of (a) 30; (b) 60; (c) 80; (d) 100; (e) 120 μJ·pulse^{-1}.

Figure S8. Integrated emission intensity as function of the stripe length of UV exposed regions in PBS1-M.

Figure S9. Spectra at the waveguide output for (a) PBS1-M and (b) PBS2-M.

Figure S10. Pulsed signals at the receiver after transmission through the waveguides in (a) PBS1-M and (b) PBS2-M.

Figure S11. Gain calculated for each channel in PBS1-M.

Synthesis and processing

Table S1 Composition, processing method and thickness of PBS-di-ureasils prepared in this study. [PBS-PFP] is the concentration of the stock PBS-PFP solution (in μM repeat units, r.u.), that is added to the d-UPTES. The weight percent (wt%) of polymer incorporated was estimated from [PBS-PFP] and the resultant mass of the dry CPE-di-ureasil.

Sample designation	[PBS-PFP] (μM r.u.)	PBS-FTP weight (%)	Processing method	Spin rate (rpm)	Thickness (mm)
dU(600)-**M**	0	0	Monolith	-	2.9
PBS1-**M**	4.7	1.2×10^{-3}		-	2.7
PBS2-**M**	98.4	1.2×10^{-2}		-	3.2
dU(600)-**F**	0	0	Film	10 000	0.82×10^{-5}
PBS3-**F**	90	2.5×10^{-2}		8 000	3.28×10^{-5}
PBS4-**F**	790	0.2		8 000	1.62×10^{-5}
PBS5-**F**	790	0.2		10 000	1.8×10^{-5}

Spectroscopic ellipsometry

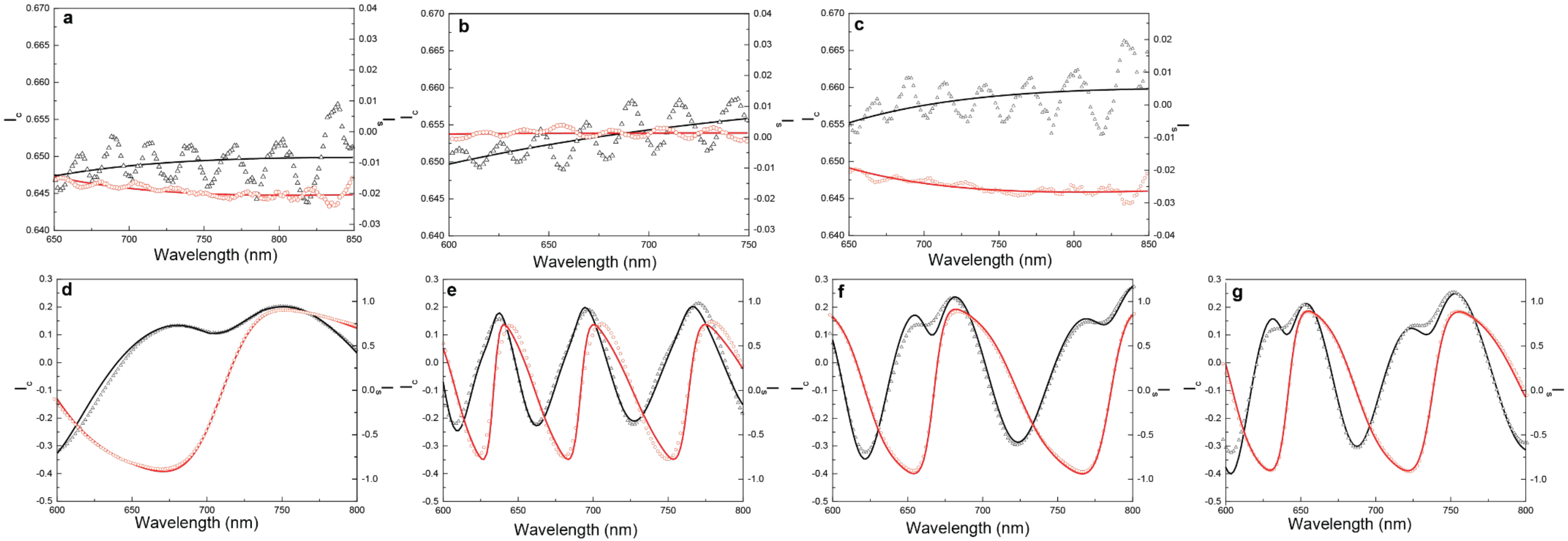

Figure S1. Ellipsometric parameters I_s (open circles) and I_c (open triangles) measured for (a) dU(600)-M; (b) PBS1-M; (c) PBS2-M; (d) dU(600)-F; (e) PBS3-F; (f) PBS4-F; and (g) PBS5-F. The solid lines represent the data best fit.

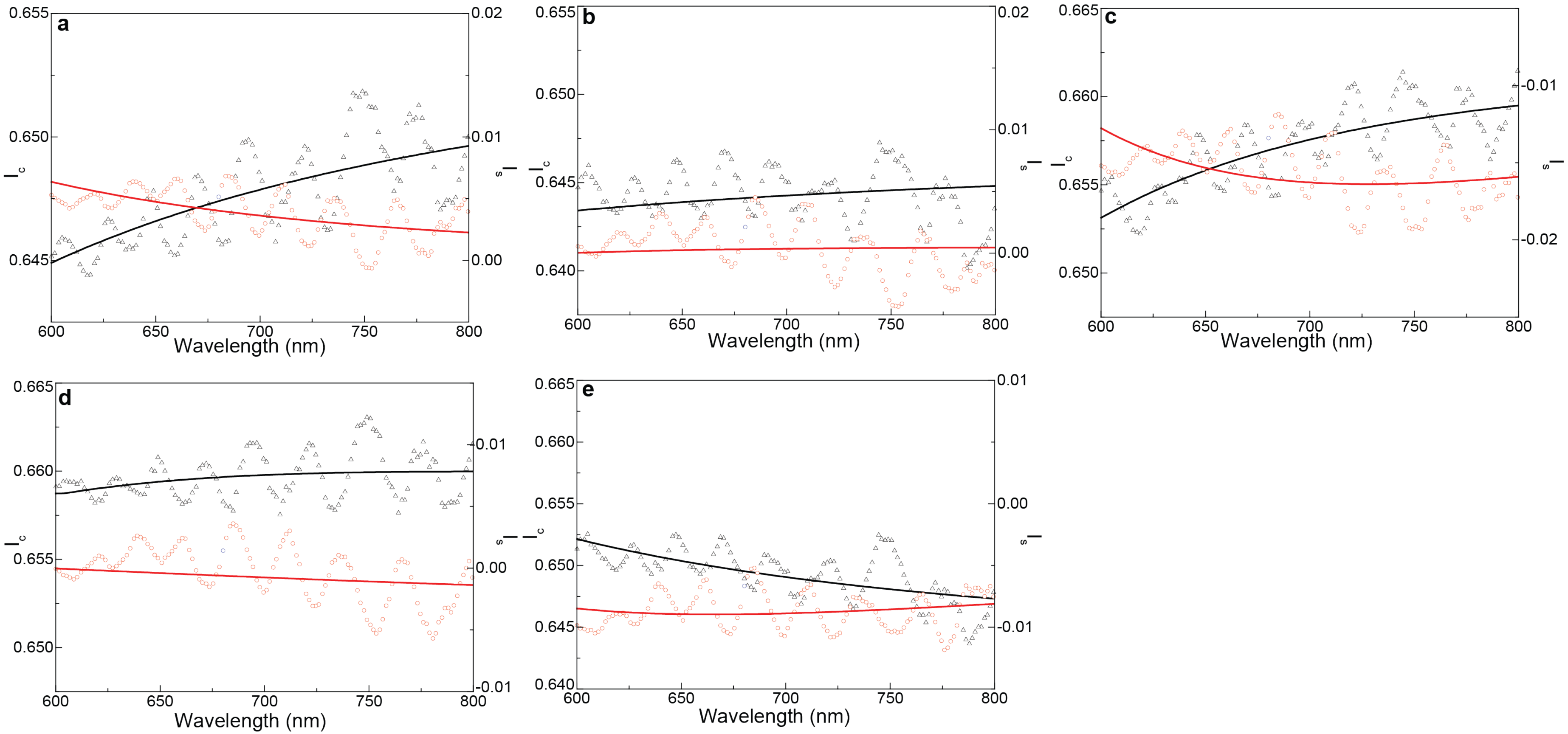

Figure S2. Ellipsometric parameters I_s (open circles) and I_c (open triangles) measured in PBS1-M in the regions exposed to UV radiation with energy of (a) 30; (b) 60; (c) 80; (d) 100; (e) 120 μJ·pulse^{-1}. The solid lines represent the data best fit.

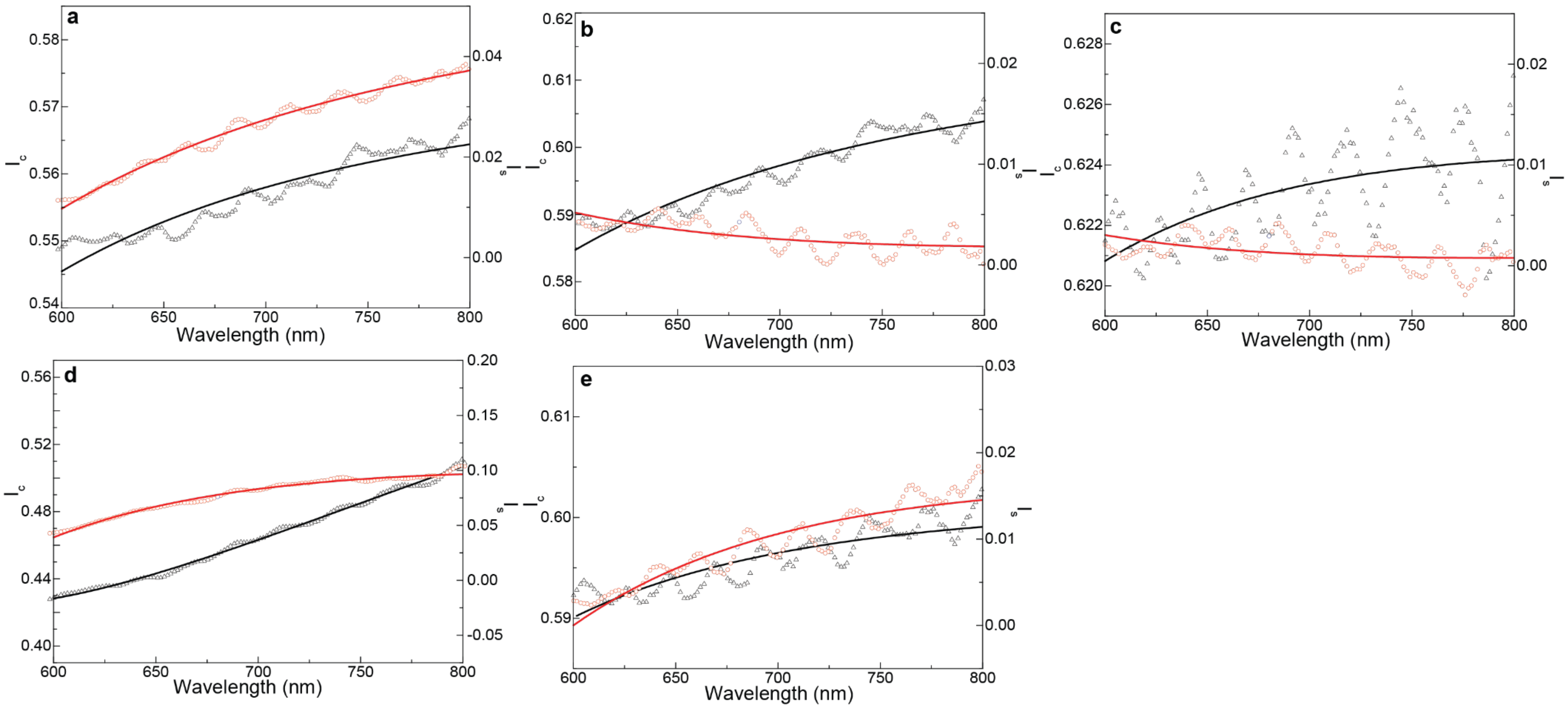

Figure S3. Ellipsometric parameters I_s (open circles) and I_c (open triangles) measured in PBS2-M in the regions exposed to UV radiation with energy of (a) 30; (b) 60; (c) 80; (d) 100; (e) 120 μJ·pulse^{-1}. The solid lines represent the data best fit.

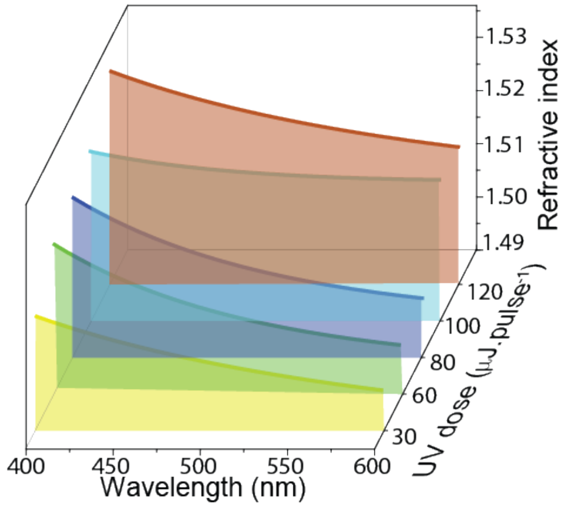

Figure S4. Dispersion curves obtained for the channel waveguide regions in PBS1-M.

Optical measurements

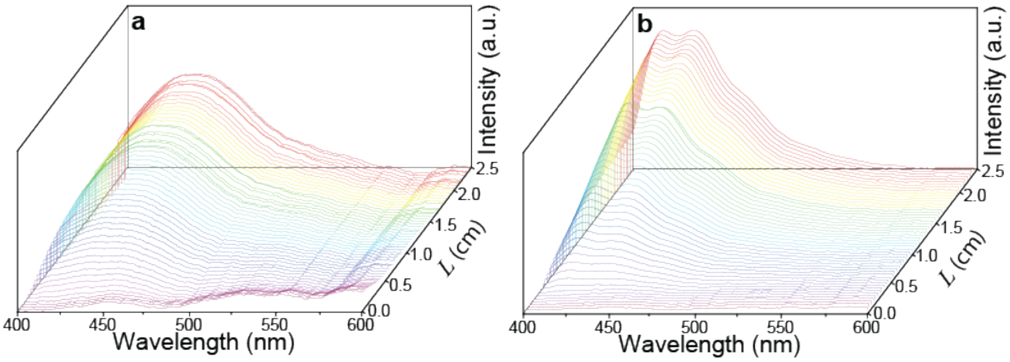

Figure S5. Emission spectra for different stripe lengths in (a) dU(600), (b) PBS1-M.

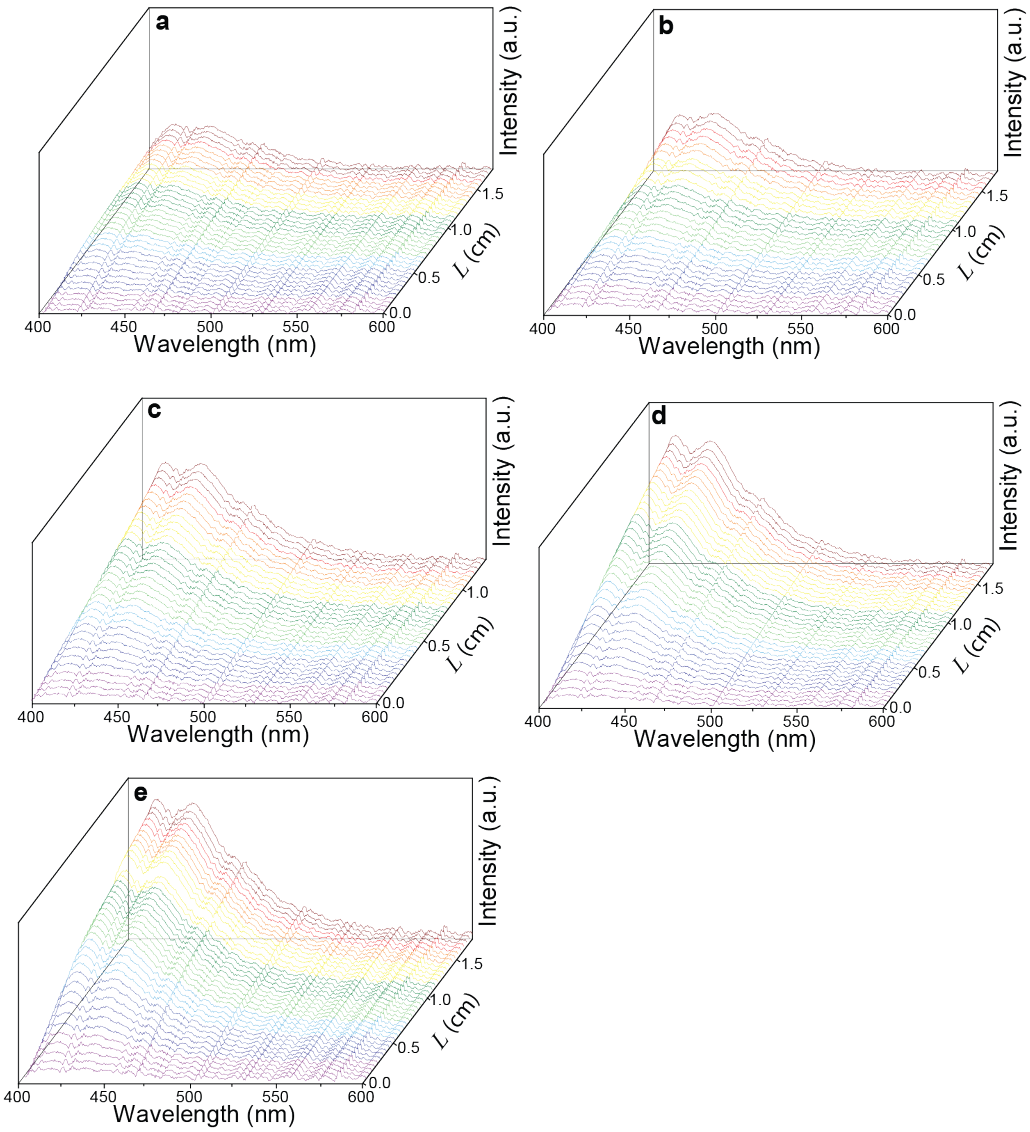

Figure S6. Emission spectra for different stripe lengths PBS1-M in the regions exposed to UV radiation with energy of (a) 30; (b) 60; (c) 80; (d) 100; (e) 120 μJ·pulse^{-1}.

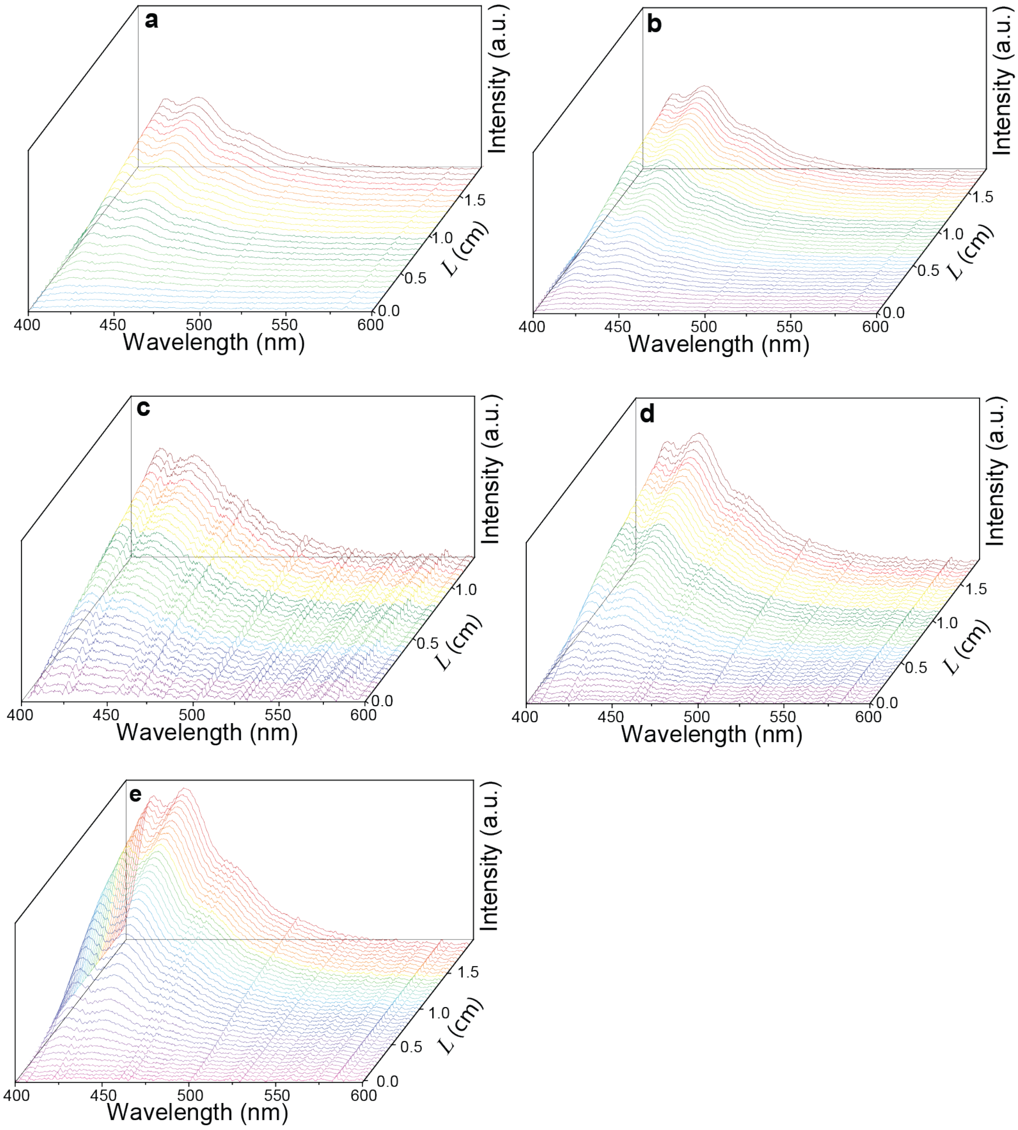

Figure S7. Emission spectra for different stripe lengths PBS2-M in the regions exposed to UV radiation with energy of (a) 30; (b) 60; (c) 80; (d) 100; (e) 120 μJ·pulse^{-1}.

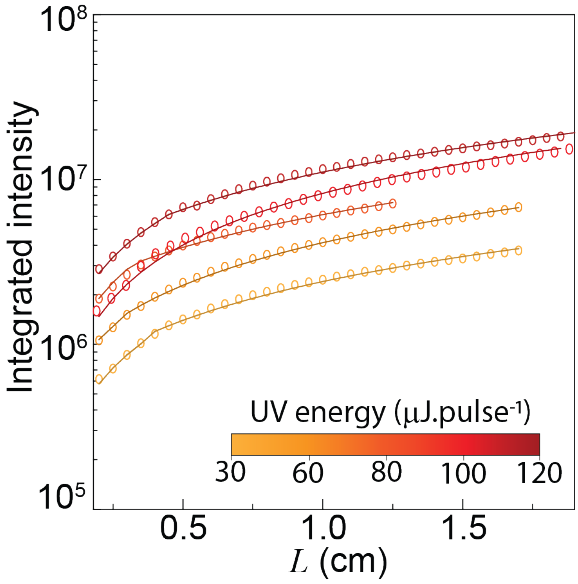

Figure S8. Integrated emission intensity as function of the stripe length of UV exposed regions in PBS1-M.

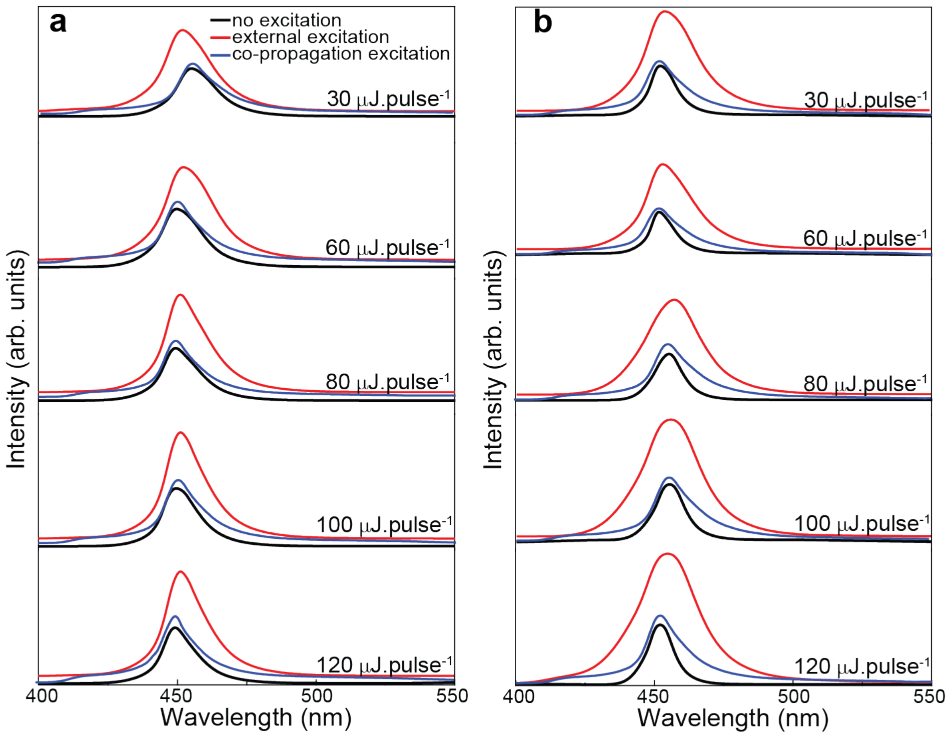

Figure S9. Spectra at the waveguide output for (a) PBS1-M and (b) PBS2-M.

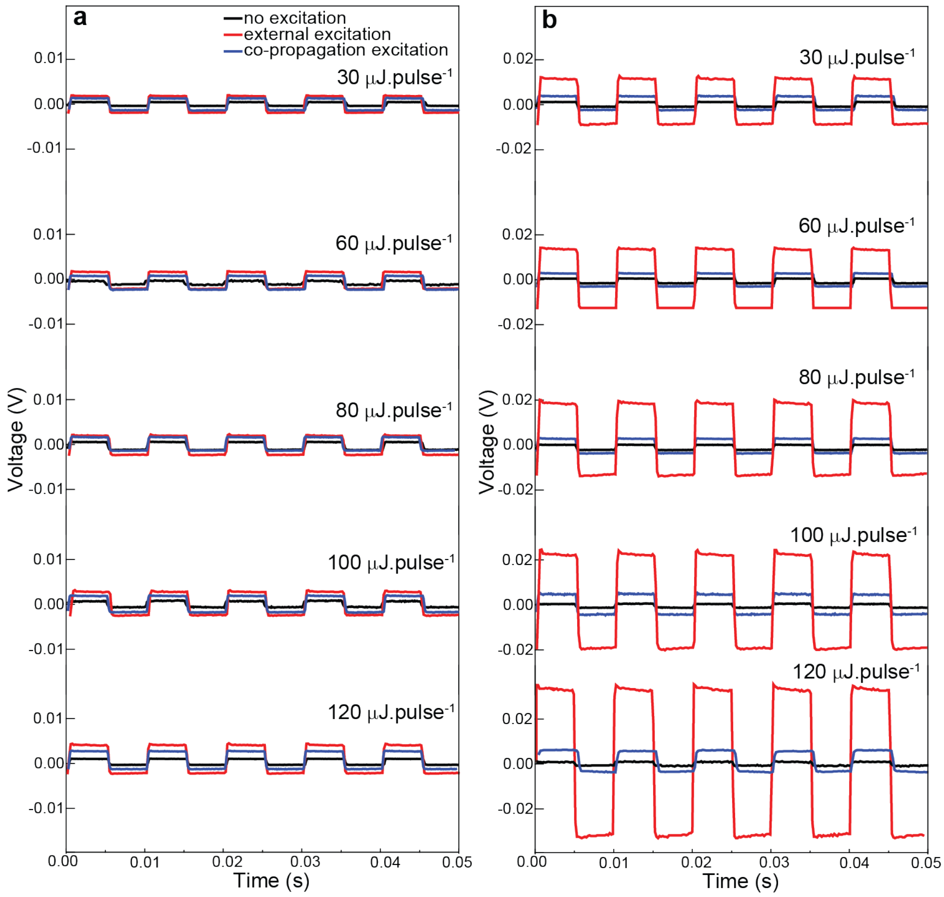

Figure S10. Pulsed signals at the receiver after transmission through the waveguides in (a) PBS1-M and (b) PBS2-M.

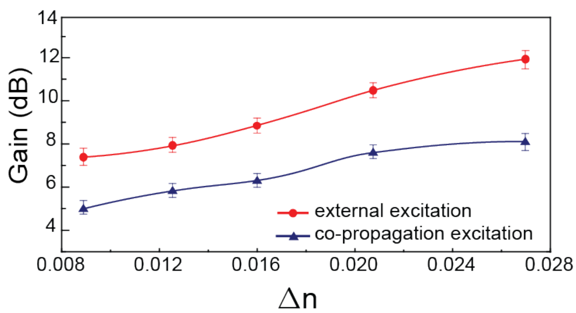

Figure S11. Gain calculated for each channel in PBS1-M.